EPJ Web of Conferences **302**, 14002 (2024) https://doi.org/10.1051/epjconf/202430214002
SNA + MC 2024

SiC Detector Thickness Optimization for Enhanced Response Variability

Enrica Belfiore[1*], *Rodolphe* Antoni[1], *Mehdi* Ben Mosbah[1], *Pierre-Guy* Allinei[1], and *Quentin* Potiron[2]

[1]DES/IRESNE/DTN/SMTA/Nuclear Measurement Laboratory, CEA Cadarache, 13108 Saint-Paul les Durance, France
[2]CNRS, IM2NP, Aix-Marseille University, Université de Toulon, 13284, Marseille, France

Abstract. Neutron spectroscopy is a crucial point in several nuclear applications. Accurately measuring fast neutron energy distributions in high-flux conditions reveals a significant technology gap, hindering the acquisition of precise energy fluence distributions. This project investigates the potential of machine learning to bridge this gap, focusing on neutron energies from 100 keV to 20 MeV and fluence rates from $10^{10}\,\frac{n}{cm^2 s}$ to $10^{12}\,\frac{n}{cm^2 s}$ using solid detectors such as Silicon Carbide (SiC) and Chemical Vapor Deposition (CVD) diamonds. This paper details the simulation design phase of our project, emphasizing the exploration of optimal SiC solid detector thickness to introduce crucial variability for machine learning training.

1 Introduction

Neutron spectroscopy holds substantial significance within various scientific and technological domains, particularly in tasks related to beam characterization in particle accelerators and the development of methods for controlling neutron energy distribution within reactors. Also notable are applications encompassing hazardous material detection, radiation protection, neutron control in fusion reactions and nuclear spectrum measurements, including flux monitoring [1]. Presently, for the energy range of fast neutrons, there exists a technology gap concerning neutron spectrometry under conditions of high flux, hindering the acquisition of energy fluence distributions. In this context, combining resilient and accurate sensors with Machine Learning (ML) emerges as a promising approach to developing predictive models of neutron energy distributions and advancing the design of compatible detectors [2].
The feasibility of this approach has already been demonstrated through the utilization of a ML algorithm based on the unfolding of the fluence spectrum from the micro-dosimetric spectrum, which is measured by a Tissue Equivalent Proportional Counter (TEPC) gas detector in [3]. In this work, the energy deposition spectrum in the counter gas, generated by secondary charged particles interacting with the tissue-equivalent wall of the detector, was

* Corresponding author: enrica.belfiore@cea.fr

post-processed to extract micro-dosimetric information. The neutron energy range considered in the TEPC case spanned from 50 keV to 20 MeV, at a theoretical fluence rate of $10^6 \frac{n}{cm^2 s}$. However, it is important to note that this type of detector was found to be incompatible with measurements involving higher neutron fluxes. Our current project endeavours to harness the capabilities of ML while focusing on a different energy range, specifically neutron energies ranging from 100 keV to 20 MeV and fluence rates spanning between $10^{10} \frac{n}{cm^2 s}$ and $10^{12} \frac{n}{cm^2 s}$. The main detectors that can withstand this harsh environment are solid detectors [4]. This project represents a collaborative effort between the Department of Nuclear Techniques (DTN) and Department of Reactor Study (DER) - CEA departments, conducted within the framework of INSNU project. Its primary objective is the development of innovative detectors and methodologies capable of withstanding high neutron fluxes and providing spectrometric data within reactor pit environments. The five steps considered to succeed in our project are: 1. Solid detector simulation design; 2. Preparation of the data for ML approach (base-training and base test databases); 3. Selection of ML algorithm; 4. Train and test models, checks of its accuracy; 5. Validation of the algorithm with experimental results. This paper describes the simulation design phase. The primary objective of this stage is to investigate the optimal thickness of a solid detector, enabling the attainment of the widest possible variability. In ML terminology, a substantial variability is crucial for enriching the dataset with a diverse array of scenarios, thus enabling the algorithm to train on a comprehensive set of possibilities. For this project the solid detectors were considered. These detectors, with silicon being a commonly employed material, possess inherent resilience and durability, rendering them particularly suitable for deployment in challenging nuclear environments. The most commonly available solid detectors are Silicon-Carbide (SiC) and diamond-based (CVD diamond) detectors. The optimal thickness of CVD diamond detector was already investigated in [5], so this document focuses on SiC one. Based on the TEPC study, the micro-dosimetric formulation was adopted and described in section 2 of this document, while the description of the SiC model and the results of the thickness optimization are presented in section 3. Finally, section 4 summarizes the work and the lessons learned carrying on this study.

2 Method

2.1 Micro-dosimetric formulation

Building upon the antecedent investigation utilizing TEPC, as elucidated earlier, the outcomes of all simulation outputs --- i.e. the deposited energy in the detector --- will be transformed into a micro-dosimetric format. The determination arose that microdosimetry proves to be a fitting methodology, furnishing adequate information to populate the ML database. Within the context of our ongoing project, a parallel analysis was conducted, although the proposition of employing deposited energy values directly has not been dismissed; rather, it is slated for subsequent exploration in alternative analyses.
Microdosimetry is the branch of radiation biophysics that studies the spatial, temporal and spectral aspects of the stochastic nature of the energy deposition processes in microscopic structures [6]. It primarily relies on the characterization of the **lineal energy** (y), a fundamental parameter defined as the energy deposited by a single event in a specified volume (ε), divided by the mean chord length of that volume ($\bar{l}$), represented mathematically as [7]:

$$y = \frac{\varepsilon}{\bar{l}} \quad (1)$$

From a microdosimetric perspective, various explanatory variables are employed to elucidate the variability inherent in each spectrum utilized for reconstructing the fluence energy distribution. Notably, the pulse-height of the sampled lineal-energy distribution of absorbed dose is employed, typically expressed in a logarithmic scale:

$$d(y) = \frac{dD}{dy} \rightarrow yd(y) \quad (2)$$

Here, y denotes the lineal energy, and the resultant $yd(y)$ distribution is commonly referred to as the **microdosimetric spectrum**. Additionally, four other explanatory variables frequently utilized in this microdosimetric context are delineated as follows:

1. The **frequency mean lineal energy:** $\overline{y_f} = \int_0^\infty y\, f(y)\, dy$ $[\frac{keV}{\mu m}]$, corresponding to a weighted lineal energy over the frequency distribution of events $f(y)$.
2. The **dose mean lineal energy:** $\overline{y_d} = \frac{\int_0^\infty y^2\, f(y)\, dy)}{\overline{y_f}}$ $[\frac{keV}{\mu m}]$, serving as a normalized variance concerning the frequency mean, providing an approximation of the mean stopping power of secondary charged particles.
3. The dimensionless parameter **alpha**: $\alpha = \frac{\overline{y_f}\, d(\overline{y_f})}{\overline{y_d}\, d(\overline{y_d})}$ [-] offers an indication of the distance between the frequency mean and the stopping power.
4. Finally, the parameter **beta**: $\beta = \frac{\overline{y_d} - \overline{y_f}}{\alpha}$ $[\frac{keV}{\mu m}]$, providing an estimation of the presence of alpha and recoil ions bump in the context of TEPC measurements.

2.2 SiC PHITS detector model

During this stage of our project, the detector configuration adopted involved modelling a SiC detector as a parallelepiped with variable thickness and a fixed height of 4 mm. To simulate the behaviour of this detector several Monte Carlo (MC)-based codes can be employed. In our project, the selection of the appropriate MC tool is pivotal. Initially, in this paper it is required to determine the detector's response and conduct parametric studies to assess the optimal thickness of the detector, and subsequently to build the ML database. At the beginning, the SiC detector model's behaviour was scrutinized using the MCNP code [8], since it is considered as the reference tool for neutron transport simulations below 20 MeV. However, this code was deemed unsuitable for the analysis as it failed to reproduce some fundamental expected physical processes in terms of production and energy deposition of secondary charged particles. Following a previous validation study conducted at DTN – CEA department on CVD detector, the PHITS code demonstrated efficacy, especially in secondary charged particles production and energy loss [9]. Consequently, the analysis continued with the SiC detector model using PHITS. It is a general-purpose MC particle transport simulation code developed in FORTRAN. This simulation code offers transport and collision capabilities for nearly all particles across a wide energy range (from 10^{-4} eV to 1 TeV/n) through Monte Carlo methods [10]. In addition, for the SiC detector model, the decision was made to exclusively address the depleted layer of the SiC detector, excluding considerations for Ohmic resistance or Schottky contact. This deliberate exclusion stems from the anticipation that the envisaged reactions will predominantly occur within this designated volume, termed the sensitive volume. This approach facilitates an assessment of the PHITS capabilities in accurately representing these reactions. To further streamline the model, a simplification was implemented, assuming a pure SiC detector composition comprised of 50% Carbon atoms and 50% Silicon atoms, devoid of impurities. The elemental composition in its natural state is detailed in Table 1. This simplified representation aids in evaluating the performance of the PHITS code in scenarios where impurities are negligible, ensuring a focused examination of the fundamental SiC detector characteristics.

Table 1. Natural composition of Si and C atoms [11].

Isotope	Abundance [%]
^{12}C	99.9
^{13}C	0.1
^{28}Si	92.2
^{29}Si	4.7
^{30}Si	3.1

50,000,000 particles distributed across 10 batches were systematically considered in our simulation. This selection was made with the objective of achieving a judicious balance between computational efficiency and the attainment of reliable statistical precision. In concert with these considerations, the energy grid underwent subdivision into 1500 energy bins, distributed logarithmically. The Fano Factor and resolution parameters, pivotal for accurate simulation outcomes, were established based on literature findings, setting their values to 0.1 and 0.012, respectively, as per the work by [12]. All requisite nuclear data were taken from the JENDL-4.0 library [13], which serves as the default nuclear data library in the PHITS code.

2.3 Thickness optimization to get the maximum variability

To ascertain the *optimal thickness* of the SiC detector, a comprehensive parametric analysis was conducted. The optimization procedure aimed to evaluate the detector thickness that maximizes variability. Based on the CVD diamond study, a total of 10 spectra and 8 distinct thicknesses were incorporated into the analysis. Among the 10 spectra considered, five were characterized as monoenergetic, while the remaining five were sourced from the IAEA Compendium database [14]. This document serves as a repository, providing a comprehensive collection of measured, realistic, laboratory and standard neutron spectra. The selection of these spectra was strategically performed to encompass the entire range of interest, incorporating variations in spectral shapes. The specific spectra chosen to fulfill this objective are outlined below and visually depicted in Figure 1:

- Am-Be source;
- Boiling Water Reactor (BWR) -excore location;
- 14 MeV streaming, from fusion reactor work place;
- Photoneutrons from 14 MeV photons in tungsten + 90 cm concrete, from medical accelerator applications;
- 5 tonnes natural U pile, from nuclear material processing facility.

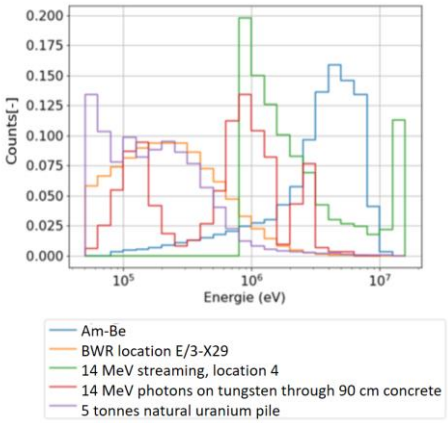

Fig. 1. Selected spectra from the IAEA Compendium database.

In opposite, the selection of the monoenergetic spectra was done discriminating the contribution of the different possible reactions, exploiting the threshold energy reported in [15]. The monoenergetic spectra selected are:

- 1 MeV : only elastic scattering in Si and C ;
- 3 MeV : elastic scattering in C and Si, inelastic scattering in Si, $^{28}Si(n,\alpha)^{25}Mg$ reaction ;
- 5 MeV : elastic and inelastic scattering in C, elastic and inelastic scattering in Si, $^{28}Si(n,\alpha)^{25}Mg$, $^{28}Si(n,p)^{28}Al$ reactions ;
- 7 MeV : elastic and inelastic scattering in C, elastic and inelastic scattering in Si, $^{28}Si(n,\alpha)^{25}Mg$, $^{28}Si(n,p)^{28}Al$, $^{12}C(n,\alpha_0)^{9}Be$ reactions ;
- 14 MeV : all the possible reactions.

Finally, the selected thicknesses for this analysis are: 10 µm, 15 µm, 21 µm, 30 µm, 35 µm, 40 µm, 45 µm and 50 µm. The analysis commences with a nominal thickness of 10 µm, chosen to circumvent potential fabrication challenges that may arise due to their susceptibility to breakage during detector manufacturing and testing [16]. Subsequent increments of 5 µm are applied, except for the thickness of 21 µm, a dimension notably prevalent in commercial availability for this detector [12]. In addition, this detector size is under ongoing investigations by DER-CEA department [17].

In our study, gamma production, including inelastic scattering and other reactions, was considered negligible due to the very low thickness of the sensors used. We assumed that gamma interactions do not significantly contribute to the variability in the system's response because the maximum sensor thickness considered is 50 µm. At such small thicknesses, the sensor's sensitivity to gamma rays is significantly reduced. By maintaining the thickness below 50 µm, we aimed to prevent the sensor from becoming overly responsive to higher-energy photons, especially gamma rays. Our decision to limit the active volume thickness was driven by the need to achieve an optimal balance between enhancing neutron detection efficiency and reducing sensitivity to gamma radiation. Additionally, the inherently low atomic number (Z) of SiC means that it is intrinsically less sensitive to photon radiation compared to other semiconductor detectors. This results in a decreased neutron-gamma cross-sensitivity in mixed radiation fields, which is a critical feature for neutron detection in many practical applications [18].

3 Results

3.1 Microdosimectric spectra

The simulations were executed and the resultant deposited energy was computed in order to get the microdosimetric spectrum. Figure 2 shows an example of the microdosimetric spectra computed with the different thicknesses of the detectors, facing a monoenergetic neutron flux of 14 MeV, energy usually associated to nuclear fusion applications. Compliant with Equation 1, the microdosimetric spectrum necessitates the calculation of the mean chord. The mean chord $\bar{l}$ can be determined using the Cauchy theorem, asserting that for a convex body $\bar{l} = \frac{4V}{S}$, where V denotes volume and S represents surface area. While this theorem is conventionally applicable under homogeneous irradiation from 4π, in the considered scenario, the irradiation entails a unidirectional energetic flux directed towards the solid detector's surface. Despite this deviation, the Cauchy theorem remains a viable means to approximate the anticipated mean chord [19]. In this investigation, a PHITS feature with the embedded 'T-Track' card was utilized. This feature provides the average distance travelled by neutrons in the output file, effectively yielding the mean chord. Specifically, the mean chord in case of 10µm SiC detector thickness was determined to be 15 µm using this approach, as opposed to the 19 µm calculated through the Cauchy theorem.

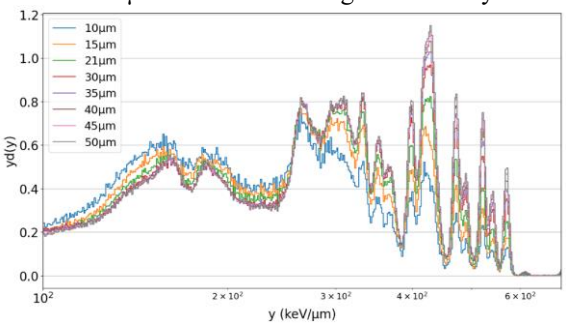

Fig. 2. Microdosimetric spectra computed with different thicknesses.

Usually the graphical representations of microdosimetric spectra can offer enhanced insights into the system's sensitivity to various charged particles, facilitated by the log-scale presentation of lineal energy.
The peak positions and intensities of the deposited energy and microdosimetric spectra were compared with values available in the literature, revealing a commendable concordance. [20, 21]. This alignment underscores the reliability of the collected data. Consequently, in the validation analysis of the PHITS code, it is discerned that all anticipated interactions are faithfully replicated. This affirmation underscores PHITS as a judicious tool for subsequent analyses involving the SiC detector.

3.2 Distance evaluation

In this section the results of the parametric analysis were reported. To perform a comparison among the computed results with the different thicknesses of the detector and the different spectra, it was decided to evaluate the distances among three selected vectors:

- The first one incorporates all the energy bins of the microdosimetric spectra obtained;
- The second one includes the four microdosimetric explanatory averaged quantities explained in section 2 ;
- The last vector is a combination of the previous two.

Prior to conducting distance calculations using various metrics, it is imperative to ensure the comparability of different components within the vector. Specifically, each microdosimetric band typically exhibits a range between 0 and 1.5, although certain microdosimetric variables may exhibit values exceeding 10. Consequently, the calculation of distances between two vectors predominantly hinges on these four microdosimetric variables. Moreover, certain machine learning algorithms necessitate the scaling of variables to ensure their proper functionality, such as neural networks. To address this issue, we explored the scaling methods available in the *StandardScaler* from the *sklearn.preprocessing* python package [22], before embarking on the distance calculations using each metric. The process of standardization, as executed through the utilization of the *StandardScaler*, can be succinctly expressed as follows: $z_i = \frac{x_i - \mu}{\sigma}$, where x_i indicates each value of the vector, μ signifies the mean value which is subtracted from each individual data point in the distribution and σ symbolizes the standard deviation. This procedure effectively centers our sample data around a mean value of zero and standardizes it to possess a standard deviation of one. After this, the obtained vectors are compared performing the distance evaluation. The distance among these vectors gives us an estimation of the variability, expressing the diversity of the cases. This means that the best thickness for our purpose will be the one with the largest distances among the different vectors. In order to conduct a comprehensive comparative analysis across all pairs of spectra, it was necessary to select a metric to evaluate the distance that is highly relevant in the context of the three distinct types of vectors employed. Subsequently, we established a foundation encompassing the calculation of distances between all pairs of spectra for each thickness, employing the aforementioned three vector types, while utilizing various metrics available in the *Scipy* python library. At the end, the Euclidean distance was selected to keep the consistence with the approach done in case of CVD diamond detector. The Euclidean distance computes the square root of the sum of the squares of the differences between corresponding coordinates of the two points. The result is a non-negative value that quantifies the length of the shortest path between the two points in Euclidean space. An example of the distance evaluated with this metric is reported in Figure 3 for the three different vectors. 6 different couples were selected for this example and they are reported in the graphs with the label referring to the different neutron sources though which the detector is subjected.

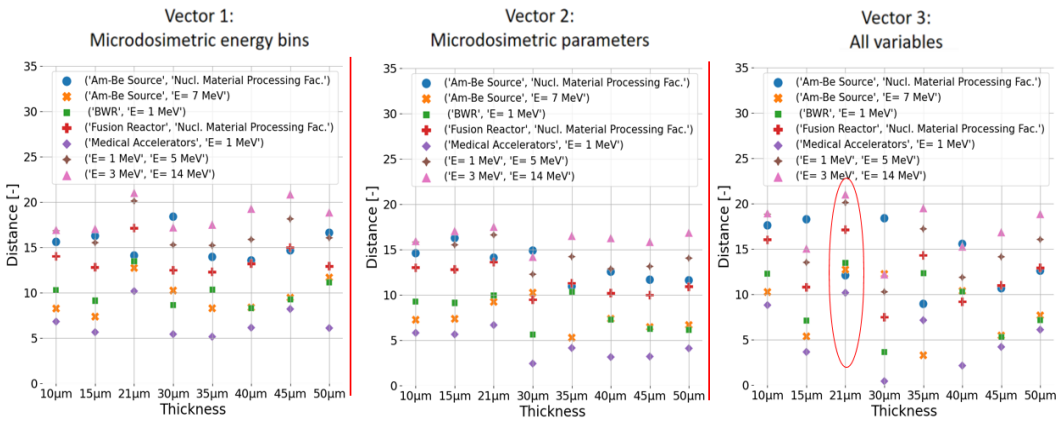

Fig. 3. Example of distance evaluations comparing the vectors obtained from the simulations of SiC detectors**.**

This means that the second pair in the scatter diagram refers to the distance calculated by comparing the microdosimetric response obtained from a SiC detector subjected to the

spectrum of Am-Be source from IAEA Compendium and one subjected to a 7 MeV monoenergetic neutron flux. The outcomes of this analysis reveal a nuanced impact of SiC detector thickness on the system's variability, contrary to the case of CVD diamond. A slightly higher distance (or better variability) was observed in case of SiC detector with 21 µm thickness, pointed out with the red oval in Figure 3.

4 Discussion

The difference in the variability of the system's response as a function of detector thickness between SiC and CVD diamond can be attributed to the significantly higher likelihood of scattering interactions with silicon nuclei across the entire energy spectrum, as compared to other interaction types. Specifically, the scattering cross-section is observed to be ten times greater than cross-sections associated with alternative interactions, and the deposited energy from ^{28}Si particles surpasses that of other particles by two orders of magnitude in our simulations. In the context of a diamond detector, one would anticipate heightened sensitivity to a broader range of potential neutron interactions with carbon atoms. This expectation arises from the comparable carbon scattering reaction cross-section with other interaction types, in conjunction with higher threshold energies for various reactions, as opposed to silicon atoms. Consequently, the CVD diamond detector system exhibits greater variability with respect to SiC due to the increased likelihood of multiple reactions: at the energy range considered, neutron interacting with a CVD detector is more likely to undergo diverse reactions, contributing to increased overall variability.
As previously mentioned, for the SiC detector under analysis in this study, a slightly higher distance was observed with 21 µm thickness. The observed phenomenon can also be attributed to the fact that particles depositing more energy typically interact within the first few micrometres of the detector, with the trajectory generally less than 20 µm, with the exception of alpha particles as illustrated in Figure 4. Protons are not depicted in the figure as they deposit only a negligible amount of energy within a 20 µm thickness of SiC. The distance covered by particles in the SiC detector depends on the kinetic energy with which they are emitted and has been calculated using the SRIM code [23]. A trajectory shorter than 20 µm implies that beyond this distance, all particles, regardless of their emission energy, come to a complete stop, resulting in a constant contribution from that point onward.

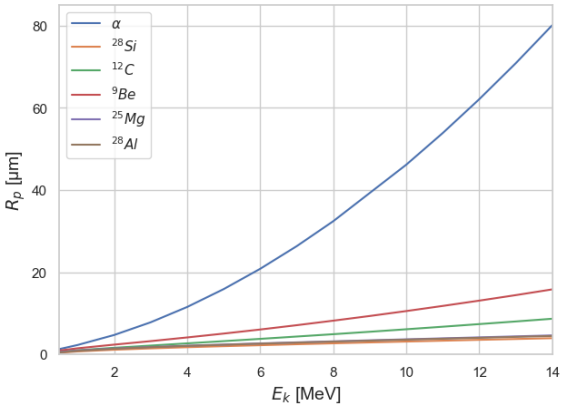

Fig. 4. Charged particles depth $\boldsymbol{R_p}$ in SiC detector after their emission at different kinetic energies $\boldsymbol{E_k}$.

In conclusion, for the above mentioned results, the thickness selected for continue further analyses on SiC detector is 21 µm. Although this is not a dimension typically explored in microdosimetry, whose conventional range of application is generally around 1 or 3 µm, the

logarithmic scale of the lineal energy improves the visibility of the gain in variability, making it a suitable choice for our study's objectives.

5 Conclusions

In this paper the preliminary simulation design phase of our project is analysed. Through Monte Carlo simulations and detailed calculations, deposited energy has been assessed and translated into a microdosimetric spectrum. This spectrum has been used to create a feature vector, which will feed a database for machine learning to predict neutron spectra. The PHITS code was employed in this analysis and its capabilities were found to well suit the purpose of reproducing the expected behaviour of CVD and SiC detectors. In particular, the latter is analysed more in detail, focusing on the thickness of it which allows a higher variability. The concept of variability is important in ML terms because it reflects the model's ability to provide different outcomes or predictions in response to different inputs or situations. To evaluate the optimal thickness, a parametric analysis was carried out by considering five mono-energetic spectra and five spectra from the IAEA Compendium database. The outputs of the various simulations were compared by calculating the distance using the Euclidean metric. The analysis demonstrates that the best detector thickness for our purpose is 21 μm. In conclusion, the study reported in this document has provided valuable insights into the design configuration and preparation of the data in view of machine learning approach. Future work prospects will include the finalization of the tests on the ML algorithm and the assessment of the impact of some assumptions behind the model, such as the choice of nuclear data library, Fano Factor and Resolution values taken among the different evaluations found in the literature. In addition, other investigations of a different SiC design will be considered. For example, the single-sphere multi-detector reported in [24]. This configuration may have the advantage to analyse different thermalized layers, which could help to increase the variability and enlarge the energy range of interest.

References

1. A. Lyoussi et al., *I_SMART a collaborative project on innovative sensor for material ageing and radiation testing: European innovative project for SiC applications in harsh media*, in CCAV, I_SMART Proposal/Exhibit 1, KIC Inno Energy, Grenoble, France (2012)

2. K. Zhou, L. Wang, L.-G. Pang and S. Shi, *Exploring QCD matter in extreme conditions with Machine Learning*, Progress in Particle and Nuclear Physics, p. 104084 (2023)

3. R. Antoni, P.-G. Allinei and L. Bourgois, *Prediction of fast neutron spectra with a spherical TEPC using a machine-learning algorithm*, Nuclear Instruments and Methods in Physics Research Section A: Accelerators, Spectrometers, Detectors and Associated Equipment, **1050**, p. 168139 (2023)

4. G. Kramberger, *Solid State Detectors for High Radiation Environments*, Particle Physics Reference Library, Springer, Cham, p. 965–1034 (2020)

5. L. Sobczak, *Dimensionnement d'un d'etecteur diamant pour la spectrométrie de neutrons rapides à partir d'une mesure micro-dosimétrique*, Rapport de stage, CEA Cadarache (2022)

6. G. A. Santa Cruz, *Microdosimetry : Principles and applications*, Reports of Practical Oncology & Radiotherapy (2016)

7. R. Antoni et al., *Microdosimetric spectra simulated with MCNP6.1 with INCL4/ABLA model for kerma and mean quality factor assessment, for neutrons between 100 keV to 19 MeV*, Radiation Measurements (2019)

8. Los Alamos Scientific Laboratory, *Group X-6. MCNP : a General Monte Carlo Code for Neutron and Photon Transport*, Dept. of Energy, Los Alamos Scientific Laboratory (1979)

9. T. Ogawa et al., New algorithm for Monte Carlo particle-transport simulation to recover event-by-event kinematic correlations of reactions emitting charged particles. In Proc. Joint Int. Conf. Math. Comput., Supercomput. Nucl. Appl. Monte Carlo Method (2015)

10. T. Sato et al., *Features of Particle and Heavy Ion Transport code System (PHITS) version 3.02*, Journal of Nuclear Science and Technology (2018)

11. *Isotopes of silicon*, Wikipedia - The Free Encyclopedia, [Online]. Available: https://en.wikipedia.org/wiki/Isotopes_of_.

12. M. De Napoli, *SiC detectors : A review on the use of silicon carbide as radiation detection material*, Frontiers in Physics (2022)

13. K. Shibata et al., *JENDL-4.0: A New Library for Nuclear Science and Engineering*, Journal of Nuclear Science and Technology, **48**, pp. 1-30 (2011)

14. R. V. Griffith et al., *Compendium of neutron spectra and detector responses for radiation protection purpose*, IAEA technical report (1990)

15. O. Obraztsova et al., *Comparing the Response of a SiC and a sCVD Diamond Detectors to 14-MeV Neutron Radiation*, IEEE Transactions on Nuclear Science, **65** (2018)

16. M. E. Wiedenbeck et al., *Thin silicon solid-state detectors for energetic particle measurements*, Astronomy & Astrophysics (2021)

17. Q. Potiron et al., *Modelling of a SiC Based Detector for the Interpretation of 14.1 MeV Neutrons Measurements*, in ANIMMA2023- The 8th International Conference on Advancements in Nuclear Instrumentation Measurement Methods and their Applications, Lucca, Italy (2023)

18. M. Hodgson et al., *Neutron detection performance of silicon carbide and diamond detectors with incomplete charge collection properties,* in Nuclear Instruments and Methods in Physics Research Section A: Accelerators, Spectrometers, Detectors and Associated Equipment, **847**, pp. 1-9 (2017)

19. P. Reuss, *Cauchy's theorem and generalization*, EPJ Nuclear Sci. Technol. , **4** (2018)

20. K. Sedlačková et al., *Properties of SiC semiconductor detector of fast neutrons investigated using MCNPX code*, in 19th Internation Conference on Applied Physics of Condensed Matter (2013)

21. R. Bernat et al., *Response of 4H-SiC Detectors to Ionizing Particles*, Crystals, **11** (2021)

22. F. Pedregosa et al., *Scikit-learn: Machine Learning in Python*, Journal of Machine Learning Research, **12**, pp. 2825-2830 (2011)

23. J. F. Ziegler, *SRIM-2003*, Nuclear Instruments and Methods in Physics Research Section B: Beam Interactions with Materials and Atoms, **219-220**, pp. 1027-1036 (2004)

24. J. M. Gomez-Ros et al., *Designing an extended energy range single-sphere multi-detector neutron spectrometer*, Nuclear Instruments and Methods in Physics Research A (2012)